Dislocation density and band structure effects on spin dynamics in GaN

Christelle Brimont, Mathieu Gallart,[a] Atef Gadalla, Olivier Crégut, Bernd Hönerlage, and Pierre Gilliot
IPCMS-GONLO Unité mixte CNRS-ULP (UMR 7504), 23 rue du Læss-BP 43-67034 Strasbourg Cedex 2, France

(Received 15 October 2008; accepted 1 December 2008; published online 20 January 2009)

We present experimental results obtained on wurtzite epitaxial GaN layers grown on sapphire and SiC substrates. Thanks to a set of samples with different values of the residual strain, we demonstrate that the high dislocation density enhances the spin relaxation rate through the Elliott–Yafet mechanism. This fact is validated by the T^{-1} temperature dependence of the spin-relaxation times. The influence of the valence-band structure on the hole-spin relaxation is also highlighted. In particular, a decrease in the hole-spin relaxation rate, accompanied by a strong polarization rate (~50%) of the differential reflectivity signal ($\Delta R/R$), is observed when the splitting ΔE_{AB} between the heavy-hole and the light-hole bands is larger than the broadening Γ_A of the A excitonic transition. On the contrary, the overlap of the A and B resonances for $\Gamma_A > \Delta E_{AB}$ is responsible for a decrease in the $\Delta R/R$ polarization rate (~10%) and an enhancement of the spin relaxation rate.
 [DOI: 10.1063/1.3056657]

I. INTRODUCTION

We have shown, in a previous paper,[1] that the high dislocation density could enhance the exciton spin relaxation rate in gallium nitride through the Elliott–Yafet[2] (EY) mechanism. These investigations of the excitonic spin relaxation in GaN were performed by using ultrafast spectroscopy techniques. Comparing our work with other experimental ones,[3,4] the major improvement from our procedure lie in the fact that the A exciton is selectively populated and that the $\Delta R/R$ signals are spectrally resolved.

We report, in the present paper, on spin dynamics measurements carried out on wurtzite GaN samples at different temperatures. These samples are provided by Lumilog® and consist of a set of epilayers, grown on different substrates and, consequently, with different residual strains, in order to study the effect of the valence band structure on spin dynamics.

We performed time- and polarization-resolved reflectivity experiments on excitons in GaN layers in a pump-and-probe configuration. According to the selection rules for excitonic optical transitions, we used circularly polarized ultrashort (~100 fs) laser pulses to achieve the optical orientation of exciton populations. Then, by analyzing the time evolution of the differential reflectivity signal as a function of polarization, we extracted the characteristic time constants for each spin relaxation channel. Thus, we were able to distinguish between the different possible relaxation processes.

II. EXCITON ENERGY AND OSCILLATOR STRENGTH DEPENDENCY ON THE SAMPLE STRAIN

The valence band structure of GaN crystals is greatly affected by strain, which can be due to a lattice mismatch between substrate and epilayer. Both the transition energy and the oscillator strength of excitons are modified.[5] Thus, by analyzing the spin dynamics in epilayers with different values of the residual strain, we expect to be able to correlate the spin physics with the valence band structure of GaN. Four specific samples are considered here. Their characteristics (exciton energies and substrate), determined by linear optical properties (photoluminescence and reflectivity in normal incidence), are listed in Table I. The sample used in our previous work (sample 1) is also included in this study.

As discussed in the literature,[5] the transition energies of the A, B, and C excitons vary continuously as a function of biaxial strain, while, for a light polarization perpendicular to the wurtzite **c**-axis, the B and C excitons exchange their oscillator strength. The oscillator strength of the A exciton, calculated in a band to band model, is not strain dependent. For fully relaxed GaN epilayers and for light propagating along the wurtzite **c**-axis, the oscillator strengths for the A, B, and C excitons would be close to 0.5, 0.3, and 0.2, respectively. For a GaN layer in biaxial compression, the energy hierarchy is the conventional one and the B exciton presents stronger oscillator strength with regard to the C exciton: this is the case for samples 1 and 2, which were grown on a sapphire substrate. On the opposite, for a GaN layer in extension, the heavy- and light-hole bands are reversed, while the oscillator strength of the C exciton increases to the detriment of the B exciton one; this is the case for samples 3 and 4. To observe this reverse ordering of heavy- and light-hole

TABLE I. substrate and transition energy of the A, B, and C excitons for the GaN samples.

Sample	Substrate	X_A (eV)	X_B (eV)	X_C (eV)
1	Sapphire	3.495	3.503	3.533
2	Sapphire	3.496	3.504	3.534
3	SiC	3.463		3.478
4	SiC	3.447		3.463

[a]Electronic mail: Mathieu.Gallart@ipcms.u-strasbg.fr.

bands, a strong tensile stress is needed. This was achieved on samples 3 and 4 grown on SiC substrate without any buffer layer. These two samples are very unique and are valuable to the conclusions drawn in this work.

The experimental procedure presented here is identical to the one done in Ref. 1 on sample 1. Optical parametric amplifiers, tuned close to 710 nm (1.746 eV), generate pump and probe pulses. Both of them are frequency doubled with two BBO crystals to reach the GaN exciton spectral region. The pulse duration is estimated to be ~200 fs. The pump pulses are spectrally filtered through a Fabry–Pérot cavity to a spectral width of $\Delta E = 5.46$ meV full width at half maximum and are tuned to achieve a resonant optical pumping of the A exciton for each sample. The probe pulses are spectrally broad and cover the two active excitonic transitions: either A and B excitonic transitions (samples 1 and 2), or those related to excitons A and C (samples 3 and 4). The two circular components of the reflected probe pulses are registered simultaneously as a function of the pump-probe delay time. For each time delay, the two reflected probe spectra are recorded in the presence and then in the absence of the pump pulse excitation and two $\Delta R/R$ spectra are calculated, one for each probe polarization ($\sigma-$ and $\sigma+$). In all measurements, the sample was held in a cold-finger cryostat at low temperatures.

Figure 1 shows typical $\Delta R/R$ spectra for the two different probe helicities at a positive time delay (pump pulse arrives before the probe pulse on the sample) of 0.2 ps for samples 2, 3, and 4. For each sample, two resonances are observed. For sample 2, they are located at 3.497 and 3.506 eV and correspond, as discussed above, to the A and B excitonic transitions, respectively. For sample 3, they are positioned at 3.461 and 3.476 eV and, for sample 4, at 3.449 and 3.465 eV. For these last two samples, these transitions correspond to the A and C excitonic transitions. As expected from the optical selection rules, the amplitude of the $\Delta R/R$ spectra, for each of the three samples (2, 3, and 4), is dependent on probe polarization. This indicates that a spin polarized population of excitons has actually been photocreated.

The spectra related to sample 2 are very similar to those obtained from sample 1 (which has been studied in our previous paper): both samples were epitaxed on a sapphire substrate and their excitonic transition energies are very close, demonstrating that the biaxial strain is equivalent for both of them. Besides, the intensity and spectral shapes of the differential reflectivity spectra are comparable for the two samples. In particular, for a contrapolarized pump and probe pulse configuration, a structure is present 6 meV below the A excitonic transition. We identified this structure as an induced exciton-biexciton transition. In a $\sigma^+\sigma^-$ configuration, the spectrum for sample 3 also presents such type of structure about 6 meV below the A excitonic transition. In sample 4, however, the large broadening of the A exciton resonance does not allow to observe this feature. As stated before, these induced exciton-biexciton transition signals disappear with the population of $|+1\rangle_A$ excitons and are not observable in a $\sigma^+\sigma^+$ configuration. These facts evidence that the loss of the $|+1\rangle_A$ excitonic population does not feed directly the $|-1\rangle_A$ pseudospin state, as it would be the case of a simultaneous

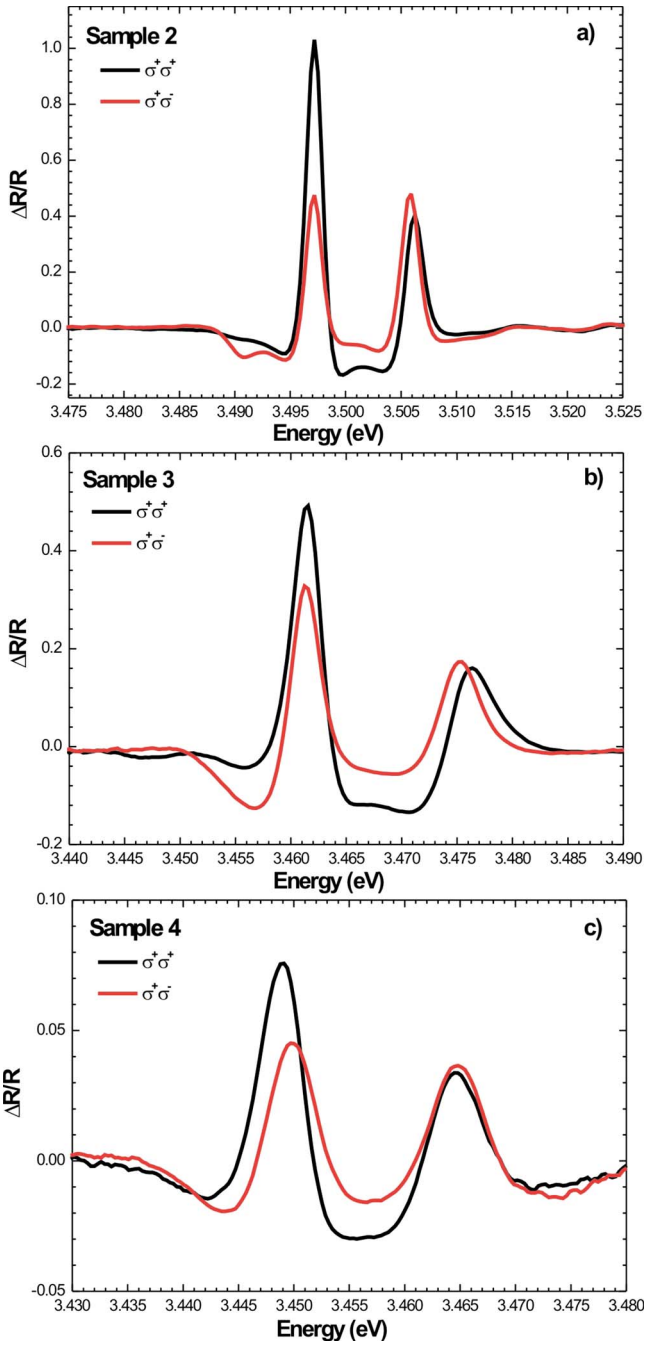

FIG. 1. (Color online) $\Delta R/R$ spectra for co- and counterpolarized configurations of the pump and probe pulses for samples 2, 3, and 4. The delay between the pump and probe pulses is 0.2 ps. The two resonances are related to the A and B excitons.

spin flip of electron and hole. In other words, samples 1, 2, and 3 show the same behavior, demonstrating that, whatever the strain, the relaxation of the exciton as a whole, where the joint electron and hole spin flips populate the $|-1\rangle_A$ state, presents a negligible contribution with respect to the spin relaxations of the individual carriers, which populate the dark $|\pm 2\rangle_A$ exciton states.[6]

III. DISLOCATION AND VALENCE BAND MIXING EFFECTS

In order to compare the experimental results, we extracted the polarization rate of the differential reflectivity sig-

TABLE II. Spin polarization rate P_C calculated from the two polarization components of the $\Delta R/R$ signal for the four studied samples of GaN.

Sample	Spin polarization rate (%)
1	52
2	38
3	18
4	12

nal, induced by the pump pulse, at zero time delay, and at the energy of the A exciton. The polarization rate is calculated from polarization changes in the right and left circularly polarized reflected probes as

$$P_C = \frac{\frac{\Delta R}{R}(\sigma^+) - \frac{\Delta R}{R}(\sigma^-)}{\frac{\Delta R}{R}(\sigma^+) + \frac{\Delta R}{R}(\sigma^-)}.$$

This amount depends on the difference between $|+1\rangle_A$ and $|-1\rangle_A$ populations, as well as on the other exciton populations (such as $|\pm 2\rangle_A$ dark states). In the case of a perfect wurtzite crystal, since the degeneracy between heavy- and light-holes bands is lifted by the crystalline field, the spin polarization can reach a theoretical value of 100%. This increase in the spin polarization rate with the splitting between heavy and light holes was also observed in uniaxially stressed cubic semiconductors.[7] The spin polarization rates for the A excitonic transition are listed in Table II.

Samples grown on sapphire substrate present a large spin polarization rate ranging from 38% to 52%. This is approximately half of the maximum values expected for a perfect wurtzite structure. On the contrary, samples epitaxed on SiC substrate display a weaker polarization rate that does not exceed 20%.

We can explain these differences by the valence band structure. To illustrate this point, we plotted in Fig. 2 the absolute value of the calculated energy splitting ΔE_{AB} between the A and B excitons (full line), as a function of the biaxial stress (the A exciton energy is also reported on the horizontal axis). Because the excitonic transitions present a finite linewidth, the probability of photocreating a B exciton population is nonzero for small values of ΔE_{AB}. For this reason, the graph also displays the broadening of the A exciton transition Γ_A, determined from the linear reflectivity spectra for the four studied samples (symbols). One can see that, for a particular value of the biaxial strain, $\Delta E_{AB}=0$, i.e., A and B excitons are degenerate: the band structure is similar as the zinc blende one. Then, a σ^+ polarized optical excitation, resonant with the A exciton, simultaneously creates $|+1\rangle_A$ excitons with an oscillator strength of 1/2 and $|+1\rangle_B$ excitons with an oscillator strength of 1/6. In reflectivity measurement, it gives rise to a spin polarization rate that we can estimate to be close to 50% at maximum. For larger splittings, P_C is supposed to increase with $|\Delta E_{AB}|$ and can theoretically reach a 100% value when the degeneracy between heavy- and light-hole bands is totally lifted. Between these two limiting situations, P_C depends on the relative proportion N_B/N_A of B and A excitons that are photocreated. In a simple model, N_B/N_A is proportional to the overlap of two Gaussian functions, with a width parameter Γ_A, centered on the A and B lines and behaves as $\exp[-(\Delta E_{AB}/\Gamma_A)^2]$.[8] The proportion of B excitons $N_B/(N_A+N_B)$, and therefore the polarization rate P_C, are a function the reduced quantity $\Delta E_{AB}/\Gamma_A$. In particular, taking into account the stress dependency of the B exciton oscillator strength,[5] the maximum value of the ratio $N_B/(N_A+N_B)$, and so the minimum value for P_C, is expected for $\Delta E_{AB}/\Gamma_A \sim 0.33$. P_C is assumed to increase monotonically for $|\Delta E_{AB}|/\Gamma_A - 0.33 > 0$. This is what we qualitatively observe in Fig. 3 where the spin polarization rate is plotted as a function of $\Delta E_{AB}/\Gamma_A$. For samples 1 and 2, $|\Delta E_{AB}|/\Gamma_A \gg 0.33$ and the spin polarization rate is large because we were able to photocreate only A excitons resonantly. For samples 3 and 4, even if ΔE_{AB} is nonzero, A and B transitions overlap because of the substantial inhomogeneous broadening. Despite a small oscillator strength, the pump pulse also creates B excitons, which leads to the low-

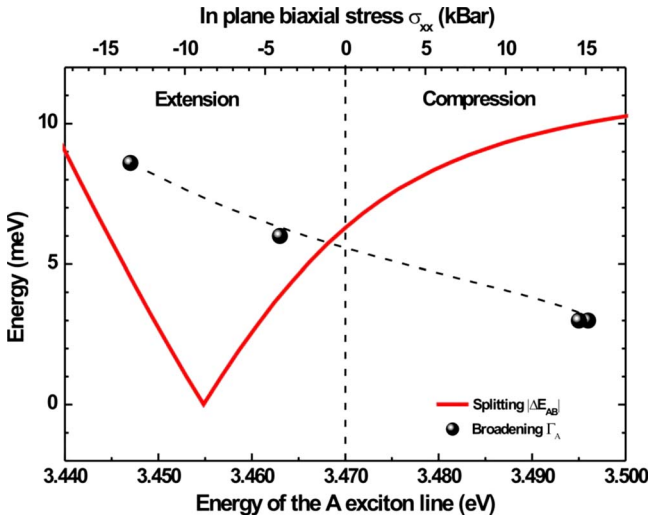

FIG. 2. (Color online) Dependence of calculated ΔE_{AB} and measured Γ_A as a function of the A exciton energy in the four GaN samples.

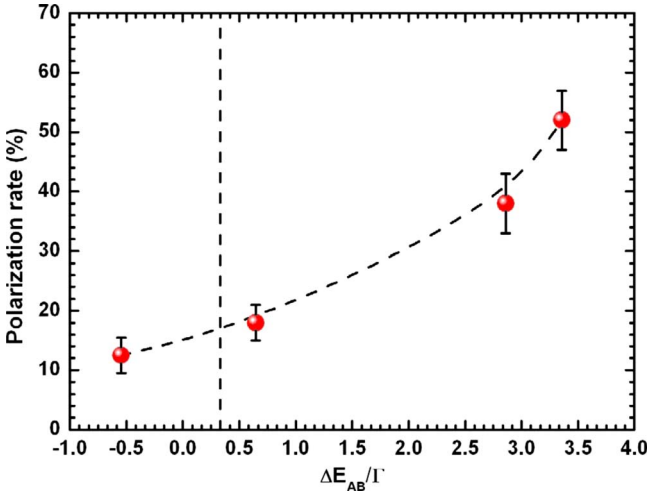

FIG. 3. (Color online) $\Delta R/R$ polarization rate as a function of the ratio $\Delta E_{AB}/\Gamma_A$. The vertical line corresponds to the specific value $\Delta E_{AB}/\Gamma_A = 0.33$ for which the polarization rate is expected to reach a minimum.

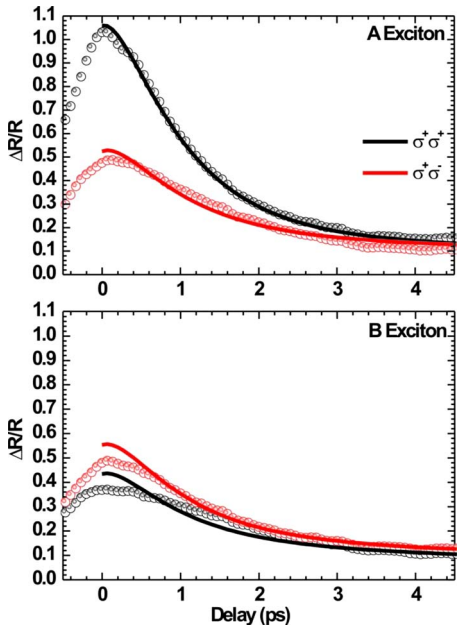

FIG. 4. (Color online) Spectrally integrated $\Delta R/R$ decays for co- and counterpolarized configurations of the pump and probe pulses. Symbols are the experimental data and full lines are the adjustments.

ering of the spin polarization rate. However, this analysis, based on a simple band to band model, does not account for the low polarization rate measured in sample 4. Moreover, the spin polarization rates are half of the expected values. Gil and Briot[9] pointed out that including the excitonic effect, and in particular the exchange interaction, reinforces the light-crystal coupling for C excitons, having Γ_5-symmetry in σ polarization, and simultaneously reduces the oscillator strength of Γ_5 B and Γ_5 A excitons. This effect is particularly significant for GaN layers in strong extension and, without any doubt, it is responsible for the low spin polarization rate of sample 4.

The spectrally integrated $\Delta R/R$ decays for the four bright excitons are displayed on Fig. 4 for sample 2 (dotted lines). For the sake of succinctness, equivalent decays for samples 3 and 4 are not shown here. Their shape is qualitatively similar to those of sample 2. However, they are different in terms of dynamics: the duration of $\Delta R/R$ signals in the case of the sample 2 is substantially identical to that measured for sample 1. After 4 ps, the relaxation of the excitonic spins for these two samples leads to an equalization of the $\Delta R/R$ signals for the two probe polarization configurations. On the contrary, equalization of the $\Delta R/R$ signals in the case of samples 3 and 4 is much faster. On a timescale shorter than 1 ps, the $\Delta R/R$ values are similar. Therefore, the samples in extension present faster relaxation dynamics than those in compression.

The whole dynamics of the system is fitted with an eight-level rate equation system, taking into account both radiative and dark excitons in their different spin configurations for the four samples. The detailed description of this procedure can be found in our previous works.[1,10] These adjustments enable us to extract the carrier spin relaxation times and population life times for the A and B or A and C excitons (Table III). An example of the adjustment is illustrated in Fig. 4 (continuous lines).

For the four samples, the electron-spin relaxation times τ_e are always longer than the pseudospin relaxation time of the holes. Moreover, the variation in τ_e as a function of the sample is less violent than the spin relaxation time of the different types of holes. This is due, roughly, to the small change in the conduction band that is induced by the different stress states between the samples. It modifies, however, deeply the valence band structure and hence the coupling between states of different J_z.

The valence and the conduction band states are mixed by the spin-orbit coupling at $\mathbf{k} \neq 0$. This last point is at the origin of the spin relaxation through the EY process.[2] Therefore, the efficiency of a scattering process between two states, initial and final, with different spins depends on two factors: the number of scattering centers and the way the states are constructed from the conduction and valence bands.

By comparing the linear optical properties of the four samples, in addition to the differences between the excitonic resonance energies, we noticed a change in Γ_A by a factor of 3. The value of this parameter reflects the crystalline quality of the GaN epilayer. It is due to the dislocations density.[11,12] During the transport, the carriers undergo scattering from threading dislocations. Many authors studied the influence of dislocation assisted scattering on electronic mobility.[13–15] The presence of such phenomena leads to a decrease in the relaxation time τ^* of the exciton wave vector and, consequently, a broadening of the electronic states. Moreover, the spin relaxation is directly linked to the wave vector relaxation. In the particular case of the EY mechanism, the spin-relaxation time τ_{spin} is proportional to the wave vector relaxation time τ^*. Jena[16] showed that, at a given sample temperature, the spin relaxation time τ_{spin}, as a function of the dislocation density N_{disloc}, yields

TABLE III. Electron, heavy-hole, and light-hole spin-relaxation times and population lifetimes of A, B, and C excitons for the four studied GaN samples.

	Relaxation times (ps)						
Sample	τ_e	τ_{hh}	τ_{lh}	τ_{so}	τ_A	τ_B	τ_C
1	15	5	1.5		1.5	3.4	
2	30	10	1.1		1	1.8	
3	7.22	2.02		0.68	0.8		0.1
4	2.06	0.16		0.02	0.15		2.6

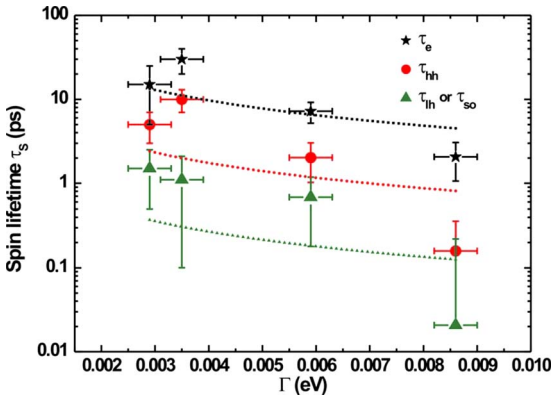

FIG. 5. (Color online) Spin relaxation times of electron, heavy, light, and splitoff holes as a function of the inhomogeneous broadening of the *A* exciton transition. The variation follows a Γ_A^{-1} law.

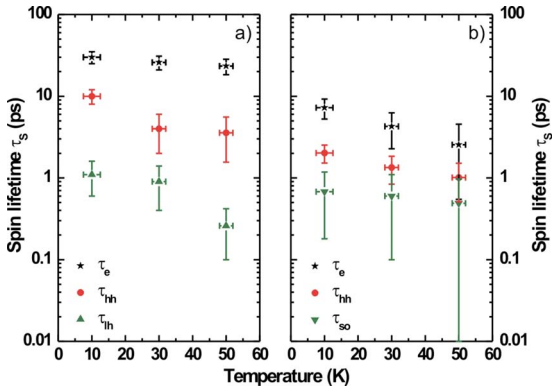

FIG. 6. (Color online) Electron, heavy-hole, and light-hole spin-relaxation times as a function of temperature for samples (a) 2 and (b) 3. The T^{-1} behavior is characteristic of a dislocation assisted EY mechanism.

$$\tau_{\text{spin}} \propto \frac{1}{N_{\text{disloc}}}.$$

In a first approximation, and as experimentally confirmed,[17] the inhomogeneous broadening varies linearly with the dislocation density. Thus, the spin relaxation time is expected to be proportional to the inverse of the excitonic transition broadening,

$$\tau_{\text{spin}} \propto \frac{1}{\Gamma}$$

Figure 5 depicts the spin relaxation time of electrons, heavy holes, and light holes (or splitoff for samples 3 and 4) for the four studied samples as a function of the excitonic transition broadening. On the same figure, the best fits using $1/\Gamma_A$ law are plotted.

Concerning the behavior of the electron-spin relaxation time τ_e, the experimental data and adjustment are in good agreement. We can understand the augmentation of the relaxation rate in terms of an enhancement of the scattering process when the density of scattering centers, i.e., dislocations, increases. The variation in the relaxation time τ_e implies that the dislocation density varies by one order of magnitude from sample 1 to sample 4. This is realistic regarding that, for heteroepitaxied wurtzite GaN, the dislocation density can vary from 10^8 to 10^{10} cm^{-2}.[18,19] Thus, the significant factor affecting the electron spin relaxation time τ_e from one sample to another is the dislocation density rather than the strength of the spin-orbit coupling. Indeed, in the electronic wave function, the mixing of the conduction state with the valence band states at $\mathbf{k} \neq 0$ is proportional to Δ_{SO}/E_g.[20] Thus, changes in the valence band structure has only little influence on Δ_{SO}/E_g taking into consideration that, in the case of GaN, $\Delta_{\text{SO}} \ll E_g$. In the conduction band, the mixing of spin-up and spin-down states is generally very low; it is therefore the importance of the dislocations density, which makes the electronic-spin relaxation efficient.

On the contrary, the evolution of the hole-relaxation dynamics, as a function of Γ_A, is more abrupt than the Γ^{-1} law used to model the experimental data. This is caused by changes in the valence band structure as a function of strain. A first consequence of this phenomenon is that we measure $\Delta R/R$ signals related to the *A* and *B* excitons for samples with compressive strain but related to the *A* and *C* excitons for samples with tensile strain. So the discontinuity for the green (triangle) curve of Fig. 5 is explained by the fact that for $\Gamma > 0.005$ eV, the relaxation time plotted on the curve is the splitoff band one and not the light-hole band one. This time may be very short (a few tens of femtoseconds) because of the strong spin-orbit coupling that exists between light and splitoff holes even for $\mathbf{k}=0$.

Concerning the heavy holes, the dynamics is accelerating when the broadening Γ_A becomes larger than the splitting ΔE_{AB}, that is to say when the light and heavy-hole bands are degenerate as it is the case for zinc blende semiconductors. The probable scattering between heavy and light holes leads to a very short spin-relaxation time, around or less than 100 fs. So, when Γ_A increases, the pseudospin relaxation by the EY process becomes more efficient for two reasons: on one hand, increasing the dislocation density increases the scattering probability of carriers and, on the other hand, the overlap of heavy- and light-hole bands increases the number of final states that are available for the relaxation mechanism.

IV. TEMPERATURE DEPENDENCY OF THE SPIN RELAXATION TIMES

In order to identify the predominant spin relaxation process occurring in our GaN samples, we performed temperature dependent experiments on samples 2 and 3. By using the same fitting procedure, we extracted the spin-relaxation time of electrons, heavy, and light holes. These data are plotted in Figs. 6(a) and 6(b) for samples 2 and 3, respectively, and for temperatures $T=10$, 20, and 50 K. A rough analysis shows that the spin relaxation times are decreasing with increasing T and the variation takes place on less than one order of magnitude. By increasing the temperature, the carrier energetic distribution is modified and the scattering probability between states with different wave vectors is enhanced. Since spin dynamics, because of the spin-orbit interaction, is strongly dependent on the wave vector relaxation dynamics, increasing the temperature affects also the spin relaxation times. By comparing the experimental evolution of spin dynamics with temperature with the expected temperature variation in the main spin-relaxation mechanisms, we can

identify which of them is responsible for the relaxation in GaN. The weak dependence with temperature would suggest the Bir–Aronov–Pikus[21] process. However, we demonstrated that this mechanism is negligible with regard to other relaxation processes.

The temperature variations in the dislocation assisted EY and D'Yakonov–Perel (DP) (Ref. 22) mechanisms were theoretically estimated;[16] according to Ref. 16, the EY efficiency process is inversely proportional to the temperature while its DP counterpart presents a T^{-4} behavior, which would result in a modification of the spin relaxation time by more than two orders of magnitude on the considered temperature range. This is not what is experimentally observed. On the contrary, a T^{-1} law reproduces nicely the experimental evolution.

V. CONCLUSION

Using ultrafast spectroscopy techniques, we investigated the excitonic spin relaxation in GaN epilayers grown by metal organic chemical vapor deposition. Experiments were carried out on a set of samples grown on sapphire and SiC substrates.

We show that the valence-band structure has a strong influence on the hole-spin relaxation. In particular, we measure that the hole-spin relaxation is slowed down when the splitting ΔE_{AB} between the heavy-hole and the light-hole bands is larger than the broadening Γ of the excitonic transitions. In this case, a strong $\Delta R/R$ polarization rate (50%) is also determined. On the contrary, when $\Gamma > \Delta E_{AB}$, the A and B resonances overlap and the system is equivalent to a zinc-blende structure where the top of the valence band is fourfold degenerate. The $\Delta R/R$ polarization rates are then weaker ($\sim$10%) and the spin relaxation times become very short.

Taking into account that the inhomogeneous broadening is connected with the dislocation density, we demonstrated that the high dislocation density enhances the spin relaxation rate of both electron and holes through the EY mechanism. This point is further verified by the temperature dependence of the spin dynamics; in agreement with the EY mechanism, the momentum relaxation rate increases with increasing temperature making the exciton dephasing time very short. This relaxation scenario is valid for epilayers grown on both types of substrates. However, samples grown on sapphire presents a longer spin relaxation time since valence bands are better separated by the compressive strain.

The spin relaxation of free excitons in bulk GaN is thus mainly caused by dislocation scattering. Therefore, to slow down the spin dynamics implies to avoid dislocations, which are always present in GaN, due to the lack of lattice matched substrates. Our work shows that, by localizing the excitons on a size scale smaller than the mean distance between dislocations, scattering can be avoided and spin relaxation inhibited. Wide bandgap semiconductor quantum dots show large confinement and exciton binding energy.[23] In this context, nanostructures, such as GaN/AlN quantum dots, are very promising for spin manipulation on long time scales.

[1] C. Brimont, M. Gallart, O. Crégut, B. Hönerlage, and P. Gilliot, Phys. Rev. B **77**, 125201 (2008).
[2] R. J. Elliott, Phys. Rev. **96**, 266 (1954); Y. Yafet, Solid State Phys. **14**, 1 (1963).
[3] T. Kuroda, T. Yabushita, T. Kosuge, A. Tackeuchi, K. Taniguchi, T. Chinone, and N. Horio, Appl. Phys. Lett. **85**, 3116 (2004); H. Otake, T. Kuroda, T. Fujita, T. Ushiyama, A. Tackeuchi, T. Chinone, J.-H. Liang, and M. Kajikawa, *ibid.* **89**, 182110 (2006).
[4] T. Ishiguro, Y. Toda, and S. Adachi Appl, Phys. Lett. **90**, 011904 (2007).
[5] B. Gil, F. Hamdani, and H. Morkoç, Phys. Rev. B **54**, 7678 (1996).
[6] For sake of simplicity, we denote by hole "spin" the projection along the growth axis of the total angular momentum J_z since the valence band spin is no longer a good quantum number because of the spin-orbit interaction.
[7] G. Lampel, A. N. Titkov, and V. I. Safarov, in *Proceeding of the 14th International Conference on the Physics of Semiconductors*, Edinburgh, edited by B. L. H. Wilson (IOP, Bristol, 1978), p. 1031.
[8] Assumption is made here that the inhomogeneous broadening of B exciton is of the same order of magnitude as Γ_A.
[9] B. Gil and O. Briot, Phys. Rev. B **55**, 2530 (1997).
[10] T. Ostatnický, O. Crégut, M. Gallart, P. Gilliot, B. Hönerlage, and J.-P. Likforman, Phys. Rev. B **75**, 165311 (2007).
[11] D. Kapolnek, X. H. Wu, B. Heying, S. Keller, B. P. Keller, U. K. Mishra, S. P. DenBaars, and J. S. Speck, Appl. Phys. Lett. **67**, 1541 (1995).
[12] F. A. Ponce, D. Cherns, W. T. Young, and J. W. Steeds, Appl. Phys. Lett. **69**, 770 (1996).
[13] D. Zanato, S. Gokden, N. Balkan, B. K. Ridley, and W. J. Schaff, Superlattices Microstruct. **34**, 77 (2003).
[14] D. C. Look and J. R. Sizelove, Phys. Rev. Lett. **82**, 1237 (1999).
[15] H. W. Choi, J. Zhang, and S. J. Chua, Mater. Sci. Semicond. Process. **4**, 567 (2001).
[16] D. Jena, Phys. Rev. B **70**, 245203 (2004).
[17] J. C. Zhang, D. S. Jiang, Q. Sun, J. F. Wang, Y. T. Wang, J. P. Liu, J. Chen, R. Q. Jin, J. J. Zhu, and H. Yang, Appl. Phys. Lett. **87**, 071908 (2005).
[18] S. D. Lester, F. A. Ponce, M. G. Craford, and D. A. Steigerwald, Appl. Phys. Lett. **66**, 1249 (1995).
[19] X. H. Wu, P. Fini, S. Keller, E. J. Tarsa, B. Heying, U. K. Mishra, S. P. DenBaars, and J. S. Speck, Jpn. J. Appl. Phys., Part 2 **35**, L1648 (1996).
[20] J. N. Chazalviel, Phys. Rev. B **11**, 1555 (1975).
[21] G. L. Bir, A. G. Aronov, and G. E. Pikus, Zh. Eksp. Teor. Fiz. **69**, 1382 (1975) Sov. Phys. JETP **42**, 705 (1976).
[22] M. I. D'yakonov and V. I. Perel', Zh. Eksp. Teor. Fiz. **65**, 362 (1973).
[23] J. Valenta, J. Moniatte, P. Gilliot, B. Hönerlage, J. B. Grun, R. Levy, and A. I. Ekimov, Phys. Rev. B **57**, 1774 (1998).